Fermilab

FERMILAB-TM-2199 March 2003

TM-2199

COUPLED-BUNCH INSTABILITIES OF THE TEVATRON AT RUN II

K.Y. Ng

Fermi National Accelerator Laboratory, P.O. Box 500, Batavia, IL 60510*

(January 17, 2003)

Abstract

The longitudinal and transverse coupled-bunch instabilities of the Tevatron at Run II are addressed in two scenarios. The first scenario corresponds to the present Run II condition: 36 proton bunches on 36 antiprotons. Each proton bunch contains 1.7×10^{11} particles with a rms bunch length 60 cm. The second scenario is for the future upgrade when there are 108 proton bunches colliding with 108 antiproton bunches. Each proton bunch contains 2.7×10^{11} particles with a rms bunch length 50 cm. Our analysis shows that the growth rates of transverse coupled-bunch instabilities are slow and will be damped by a small betatron tune spread. On the other hand, growth rates of longitudinal coupled-bunch instabilities will be fast especially for the 108-by-108 scenario.

*Operated by the Universities Research Association, Inc., under contract with the U.S. Department of Energy.

1 LONGITUDINAL COUPLED-BUNCH INSTABILITIES

1.1 SACHERER'S FORMULAS

The long-range wake left by the higher-order resonant modes of the rf cavities may couple the longitudinal motions of the bunches in the Tevatron. Assuming M bunches of equal intensity equally spaced in the ring, there are $\mu = 0,\ 1,\ \cdots,\ M_s - 1$ modes of oscillations in which the center-of-mass of a bunch leads its predecessor by the synchrotron phase $2\pi\mu/M_s$. In addition, an individual bunch in the μ-th coupled-bunch mode can oscillate in the synchrotron phase space about its center-of-mass in such a away that there are $m = 1,\ 2,\ \cdots$ nodes along the bunch longitudinally (not including the ends). For example, $m = 1$ is the rigid dipole mode, where the bunches move rigidly as they execute synchrotron oscillations, $m = 2$ is the quadrupole mode where the bunch head and tail oscillate longitudinally 180° out of phase. Actually, this has been a simplified description of the modes of perturbation inside a bunch. The full description involves another eigen-number in the radial direction.

The μ-th coupled mode will be driven if the driving narrow resonance falls on the frequency $(kM_s + \mu + m\nu_s)f_0$, where f_0 is the revolution frequency and k is an integer. For an excitation of the μth coupled mode and the mth azimuthal mode, the growth rate derived by Sacherer is [1]

$$\frac{1}{\tau_{m\mu}} = \frac{e\eta M I_b R_s f_0}{2\pi E \nu_s B_0} D F_m(\Delta\phi) \ , \tag{1.1}$$

where M is the number of bunches,[†] $B_0 = \tau_{_L} f_0$ is the *single-bunch* bunching factor with $\tau_{_L}$ being the *total* bunch length, ν_s is the perturbed synchrotron tune, R_s is the shunt impedance of the sharp driving resonance at frequency $f_r = \omega_r/(2\pi)$. The factor D is a function of the decay decrement $\alpha\tau_{\rm sep}$ between successive bunches, where $\alpha = \omega_r/(2Q)$ is the half-width-at-half-maximum (HWHM) of the resonance of quality factor Q and $\tau_{\rm sep}$ is the bunch separation. It is defined as

$$D(\alpha\tau_{\rm sep}) = -i2\alpha\tau_{\rm sep} \sum_{k=0}^{\infty} e^{-2\pi i k\mu/M - k(\alpha - i\Omega)\tau_{\rm sep}} \sin k\omega_r\tau_{\rm sep} \ , \tag{1.2}$$

[†]For a symmetrically filled ring with M_s bunches spaced n-buckets apart, the number of coupled modes is M_s, which is also equal to h/n, where h is the rf harmonic. We assume that the problem will not be significantly changed if a small fraction of bunches are missing. We therefore can have number of bunches $M \lesssim M_s$. In the 36-by-36 scenario, $n = 21$ so that $M_s = 53$, but $M = 36$.

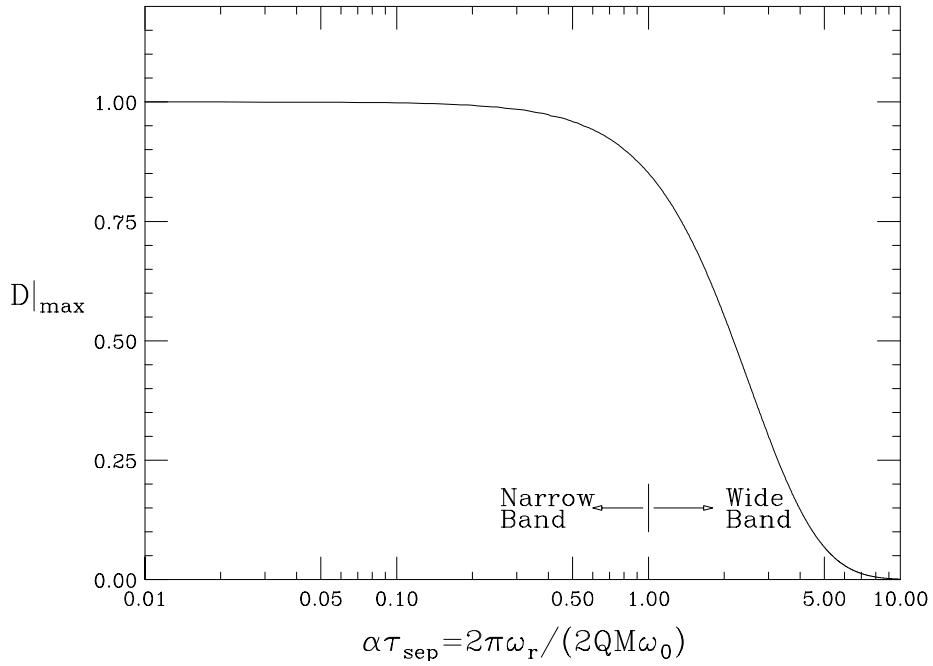

Figure 1: $|D|_{\max}$ as a function of bunch-to-bunch decay decrement $\alpha\tau_{\rm sep}$. Note that $|D|_{\max} \approx 1$ for narrow resonances but drops very rapidly as the resonance becomes broader.

The maximum magnitude of D is shown in Fig. 1. The form factor for parabolic bunches is given by

$$F_m(\Delta\phi) = \frac{16m}{\Delta\phi}\left[J_m^2(\tfrac{1}{2}\Delta\phi) - J_{m+1}(\tfrac{1}{2}\Delta\phi)J_{m-1}(\tfrac{1}{2}\Delta\phi)\right] \ , \tag{1.3}$$

where $\Delta\phi = 2\pi f_r \tau_L$ is the phase change of the resonator during the bunch passage from head to tail, and is plotted in Fig. 2. We see that mode m peaks roughly at $\Delta\phi = m\pi$. This is reasonable because, as was mentioned above, mode m represents a longitudinal variation along the bunch with m nodes (not including the ends) and it will be most easily excited when the bunch sees a phase variation of $m\pi$ of the driving resonance as it passes through the cavity gap from head to tail. Note that F_m decreases as m increases, implying that the higher m modes will not be excited so easily.

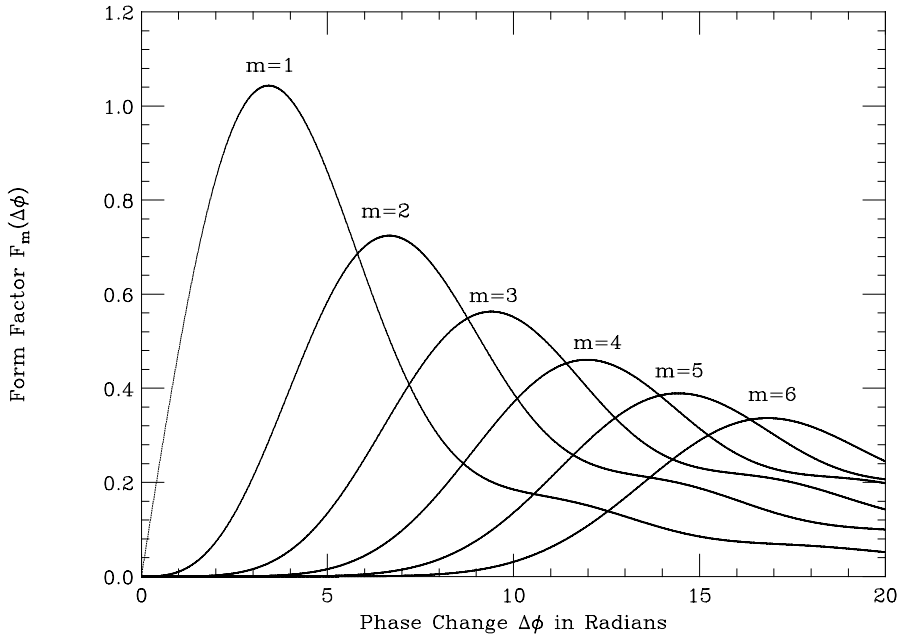

Figure 2: Form factor for longitudinal oscillation inside a bunch with $m = 1,\ 2,\ 3,\ 4,\ 5$ and 6 nodes.

1.2 THE 36×36 SCENARIO OF THE TEVATRON

The higher-order parasitic modes in the Tevatron rf cavities were measured by Sun [2] in 1995 using the method of dielectric bead pull. They were also computed using URMEL [3]. The results are listed side by side in Table I. We find that the URMEL resonant frequencies and R/Q for these modes agree rather well with Sun's measurement. On the other hand, the quality factors Q do not agree so well. This may be because URMEL computes the modes of the *bare* cavity, while some of these modes have actually been de-Qued passively. There are also a lot of structures inside the cavity and these structures have not been included in the simplified model of the cavity used in URMEL computation. In the discussions below, Sun's results will be used.

In the 36-by-36 scenario, the bunch spacing is 21 rf-buckets. If the ring is symmetrically filled, there will be $M_s = h/21 = 53$ coupled modes, where $h = 1113$ is the rf harmonic. The impedance of these higher-order parasitic resonances for one cavity is plotted in the lower trace in Fig. 3 as a function of the coupled-bunch mode μ which they will drive. The fundamental rf resonance is not included. Most of the time, the higher-order resonances of the 8 cavities will not peak at exactly the same frequencies. In this analysis, we further assume that the

Table I: Longitudinal modes for one whole cavity.

	URMEL Results			Sun's Measurements		
Mode Type	Frequency (MHz)	R/Q (Ω)	Q	Frequency (MHz)	R/Q (Ω)	Q
TM0-EE-1	53.49	87.65	9537	53.11	109.60	6523
TM0-ME-1	84.10	22.61	12819	56.51	18.81	3620
TM0-EE-2	166.56	18.47	16250	158.23	11.68	6060
TM0-ME-2	188.94	10.83	18235			
TM0-EE-3	285.94	7.53	20524	310.68	7.97	15923
TM0-ME-3	308.46	4.07	22660			
TM0-EE-4	402.69	4.93	25486	439.77	5.23	13728
TM0-ME-4	431.34	1.72	26407	424.25	1.28	6394
TM0-EE-5	511.69	5.57	25486	559.48	6.73	13928
TM0-ME-5	549.57	1.36	29453			
				748.18	10.90	13356
				768.03	2.47	16191

resonances of the 8 cavities overlap each other in such a way that the total shunt impedance remains the same as for one resonance while the total width becomes broadened (or de-Qued) 8 times.[‡] The driving impedance of all the 8 cavities are shown in the upper trace in Fig. 3. Although de-Qued, each resonance is still narrow enough to maintain a value of $|D| > 0.95$ in Eq. (1.2) if its peak falls on a synchrotron sideband. However, the resonances are broad enough to cover a number of revolution harmonics. As a result, nearly every coupled-bunch mode is affected. Above transition, the upper synchrotron sidebands correspond to growth while the lower synchrotron sidebands correspond to damping. As a result, some coupled-bunch modes will grow and some will be damped.

The growth rate for each coupled-bunch mode is computed at the injection energy of 150 GeV for each higher-order parasitic resonance. The total growth rate is obtained by summing the contribution from all the resonances. The results are listed in Table II. The injection energy was chosen because the growth rate is inversely proportional to energy and therefore the most severe instabilities will occur at the injection energy. These growth rates

[‡]If the total width is broadened only $n < 8$ times, the total shunt impedance will be increased $8/n$ times. The total number of coupled-bunch modes driven will be less; but the growth or damping rates will be faster.

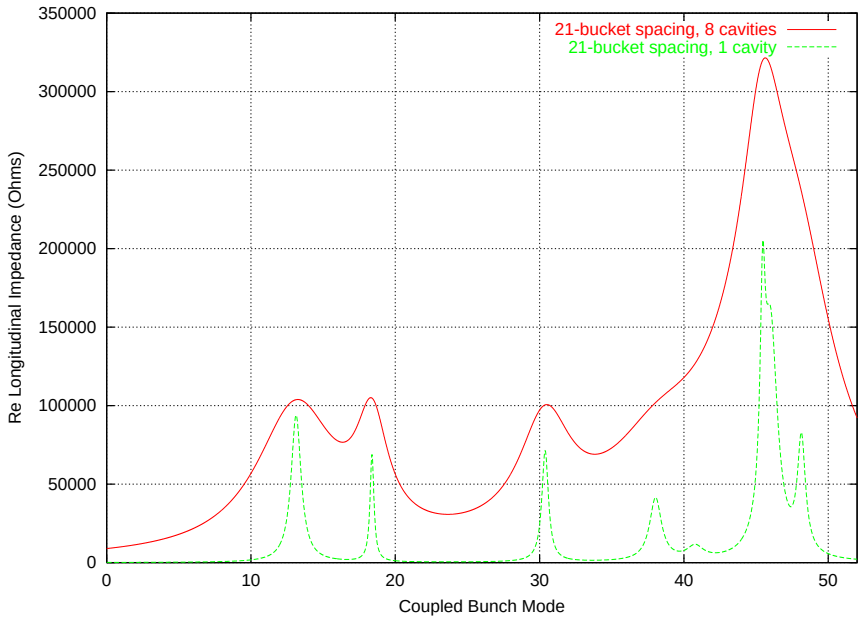

Figure 3: (color) The real part of the impedance of the higher-order parasitic resonances are plotted as a function of the coupled-bunch mode μ that they will drive. The lower (green) trace is for one cavity while the upper (red) trace corresponds to 8 cavities assuming that each resonance spread out 8 folds. The bunch spacing is 21 buckets.

and damping rates are also plotted in Fig. 4. A resonance that drives coupled-bunch mode μ will also damp coupled-bunch mode $M_s - \mu$. Thus a resonance at μ and one at $M_s - \mu$ will compensate each other for both coupled-bunch modes μ and $M_s - \mu$. Unfortunately, we do not have such matching resonance pairs in Fig. 3. As a result, as indicated in Fig. 4, the coupled modes that grow are not compensated very much by other resonances.

There is a spread of the synchrotron frequency due to the nonlinear sinusoidal rf wave form. This spread from the center to the edge of the bunch is given by

$$\frac{\Delta\omega_s}{\omega_s} = \frac{1}{16}\left(\frac{1+\Gamma^2}{1-\Gamma^2}\right)\left(\frac{h\tau_{_L} f_0}{2}\right)^2 = 0.00353 \quad \text{or} \quad \Delta f_s = 0.308 \text{ Hz} \ , \tag{1.4}$$

where the rms bunch length $\tau_{_L}$ has been taken as 60 cm, the nominal synchrotron tune $\nu_s = 1.83 \times 10^{-3}$ is assumed at the injection energy of 150 GeV with an rf voltage of 1 MV and the synchronous phase $\phi_s = \sin^{-1}\Gamma$ is taken to be zero. This spread supplies Landau damping. The mode will be stable if

$$\frac{1}{\tau} < \frac{\sqrt{m}}{4}\Delta\omega_s = 0.483\sqrt{m}\ \text{s}^{-1} \ . \tag{1.5}$$

The Landau damping rates are listed in the last row of Table V. We see that all coupled modes

Table II: Longitudinal coupled-bunch growth rates driven by the higher-order modes of the rf cavities at injection for the 36×36 scenario in Run II with rms bunch length 60 cm and bunch intensity 1.7×10^{11}.

Coupled	Growth Rate in sec^{-1}					
Bunch Mode	$m=1$	$m=2$	$m=3$	$m=4$	$m=5$	$m=6$
0	−0.549	−0.085	0.010	−0.042	0.010	−0.043
1	−0.059	−0.102	−0.171	−0.174	−0.133	−0.141
2	−0.107	−0.195	−0.272	−0.247	−0.177	−0.178
3	−0.148	−0.270	−0.374	−0.336	−0.234	−0.225
4	−0.202	−0.370	−0.500	−0.439	−0.299	−0.280
5	−0.260	−0.484	−0.613	−0.514	−0.347	−0.330
6	−0.332	−0.636	−0.710	−0.536	−0.357	−0.361
7	−0.435	−0.857	−0.832	−0.537	−0.339	−0.362
8	−0.417	−0.827	−0.770	−0.463	−0.285	−0.330
9	−0.265	−0.517	−0.507	−0.314	−0.200	−0.270
10	−0.153	−0.292	−0.308	−0.182	−0.107	−0.198
11	−0.084	−0.154	−0.174	−0.069	−0.013	−0.125
12	−0.040	−0.065	−0.082	0.021	0.067	−0.068
13	−0.013	−0.012	−0.025	0.076	0.115	−0.031
14	0.026	0.004	−0.011	0.076	0.109	−0.029
15	0.010	0.010	−0.003	0.051	0.072	−0.047
16	0.032	−0.002	−0.005	0.032	0.041	−0.057
17	0.098	−0.018	−0.018	0.009	0.016	−0.060
18	0.235	−0.029	−0.022	−0.001	0.004	−0.055
19	0.143	−0.054	−0.025	−0.006	−0.002	−0.048
20	−0.107	−0.096	−0.029	−0.008	−0.005	−0.042
21	−0.327	−0.157	−0.035	−0.009	−0.006	−0.036
22	−0.492	−0.210	−0.041	−0.009	−0.006	−0.032
23	−0.552	−0.217	−0.040	−0.009	−0.006	−0.028
24	−0.377	−0.147	−0.025	−0.002	−0.001	−0.018
25	−0.195	−0.075	−0.013	0.000	0.001	−0.014
26	−0.059	−0.024	−0.005	−0.002	−0.001	−0.002
27	0.060	0.024	0.005	0.002	0.001	0.002
28	0.195	0.075	0.013	0.000	−0.001	0.014
29	0.377	0.147	0.025	0.002	0.001	0.018
30	0.552	0.218	0.040	0.009	0.006	0.028
31	0.491	0.210	0.041	0.009	0.006	0.032
32	0.326	0.156	0.035	0.009	0.006	0.036
33	0.106	0.096	0.029	0.008	0.004	0.042
34	−0.144	0.053	0.025	0.006	0.002	0.048

Table II continued.

Coupled	Growth Rate in $\sec^{-1}$					
Bunch Mode	$m=1$	$m=2$	$m=3$	$m=4$	$m=5$	$m=6$
35	−0.235	0.029	0.022	0.000	−0.005	0.055
36	−0.097	0.018	0.018	−0.009	−0.017	0.060
37	−0.032	0.002	0.005	−0.032	−0.041	0.057
38	−0.010	−0.010	0.002	−0.052	−0.072	0.046
39	−0.026	−0.004	0.011	−0.077	−0.110	0.029
40	0.013	0.013	0.025	−0.076	−0.115	0.031
41	0.040	0.066	0.083	−0.020	−0.066	0.069
42	0.084	0.155	0.175	0.070	0.014	0.126
43	0.153	0.293	0.310	0.184	0.109	0.200
44	0.265	0.520	0.510	0.316	0.201	0.272
45	0.418	0.829	0.773	0.465	0.286	0.331
46	0.434	0.856	0.831	0.537	0.339	0.362
47	0.332	0.635	0.708	0.536	0.358	0.360
48	0.260	0.483	0.612	0.513	0.346	0.329
49	0.201	0.369	0.499	0.438	0.298	0.278
50	0.148	0.269	0.373	0.334	0.233	0.224
51	0.107	0.194	0.271	0.246	0.176	0.177
52	0.059	0.102	0.170	0.173	0.133	0.140
Laudau Damping rate (s^{-1})						
	0.483	0.684	0.837	0.967	1.081	1.184

are damped with the exception of the dipole mode ($m = 1$) in coupled modes $\mu = 30$ and 31, and the quadrupole mode ($m = 2$) in the coupled modes $\mu = 45$, 46, and 47.

We would like to point out that the stability criterion mentioned in Eq. (1.5) is a rough Keil-Schnell type criterion. The actual stability criterion is distribution dependent and is also nonsymmetric with respect to the sign of the reactive impedance. As an example, consider the inductive impedance of the vacuum chamber, which gives rise to an incoherent synchrotron frequency shift of

$$\frac{\Delta\omega_s}{\omega_s} = -\frac{3I_b\,\mathcal{I}m(Z_\parallel/n)}{2\pi^2 h V_{\rm rf}\cos\phi_s B_0^3} = -0.00684 \quad \text{or} \quad \Delta f_s = -0.595 \text{ Hz} \ , \tag{1.6}$$

where $\mathcal{I}m(Z_\parallel/n) = 3\ \Omega$ has been used. This shift is towards lower frequencies because the Tevatron is operated above transition. However, the coherent synchrotron frequency remains the same as the unperturbed synchrotron frequency f_{s0}. Thus the incoherent spread of the

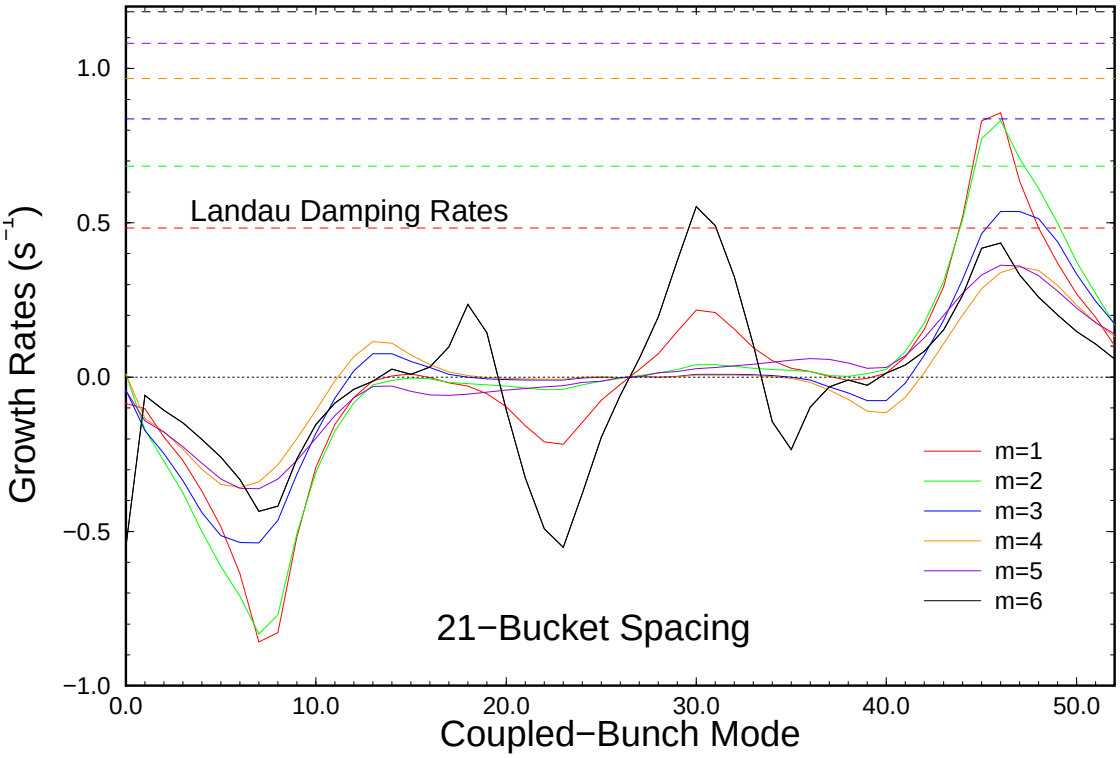

Figure 4: (color) Plot of growth rates (positive) and damping rates (negative) of each coupled-bunch mode driven by the higher-order parasitic resonances of the 8 Tevatron cavities for the 36-by-36 scenario. Landau damping rates are shown in dashes.

synchrotron frequency will not cover f_{s0}, and will not supply any damping at all. This is illustrated in Fig. 5. However, when the impedance involves a real part, it can be shown that Landau damping may exist if the real part is not too large. On the other hand, if we consider an unperturbed distribution with a vanishing gradient at the edge, the situation will be different and some Landau damping does exist even if the impedance is purely inductive. In short, more detailed solution of a dispersion relation is necessary to determine whether a certain mode is damped or antidamped.

If the growth turns out to be harmful, a fast 36×36 bunch-by-bunch damper may be necessary to damp the dipole mode ($m = 1$). A bunch-to-bunch damper for the quadrupole mode ($m = 2$) may also be necessary. This consists essentially of a wall-gap pickup monitoring the changes in bunch length and the corresponding excitation of a modulation of the rf waveform with roughly twice the synchrotron frequency.

The Tevatron bunches will be formed by coalescing 9 or more bunches in the Main Injector

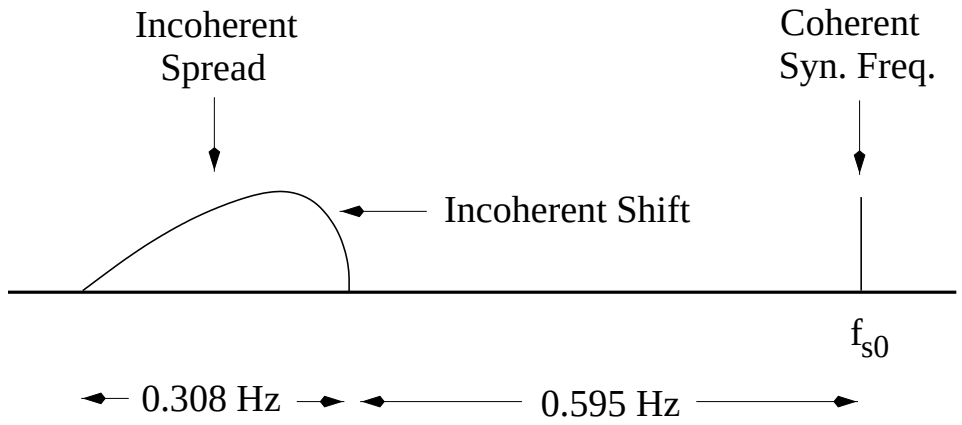

Figure 5: Schematic drawing showing the incoherent spread of $\Delta f_s \approx 0.308$ Hz is shifted by -0.595 Hz from the coherent synchrotron frequency f_{s0}, thus not being able to provide Landau damping.

(formerly in the Main Ring). Usually there will be a 10% difference in the number of particles in the final bunches. Each bunch will be experiencing a slightly different wake force and will therefore be driven slightly differently. Such broken symmetry of the coupled-bunch system will lead to some damping also.

1.3 THE 108×108 SCENARIO

We would like also to compute the longitudinal coupled-bunch growth rates for the 108-by-108 scenario. The 108 bunches are mostly at 7-bucket spacing and contain 2.7×10^{11} particles each. The rms bunch length is expected to be 50 cm. If the ring is symmetrically filled with 7-bucket spacing, there will be in total $M_s = h/7 = 159$ coupled-bunch modes. For each coupled-bunch mode, the real part of the impedance of the higher-order parasitic resonances in the rf cavities driving the coupled-bunch mode $\mu = 0,\ 1,\ 2,\ \cdots,\ 158$ are plotted in Fig. 6. The lower trace is for one cavity. The upper trace is for all 8 cavities with the assumption that the quality factors will be de-Qued 8 folds due to the fact that these resonances will not peak at exactly the same frequencies in the 8 cavities. Here, the resonances appear not as crowded as in the 21-bucket spacing in Fig. 3, the reason being that there are 3 times as many coupled modes here. We also notice that the resonances do not come in complementary pairs, i.e., μ and $M_s - \mu$. As a result, the resonances are not helping each other much in growth reduction. The growth rates at 150 GeV are computed as in the 36×36 scenario. The results are plotted in Fig. 7 for each of the 159 coupled-bunch modes. They are also listed in Table III with the

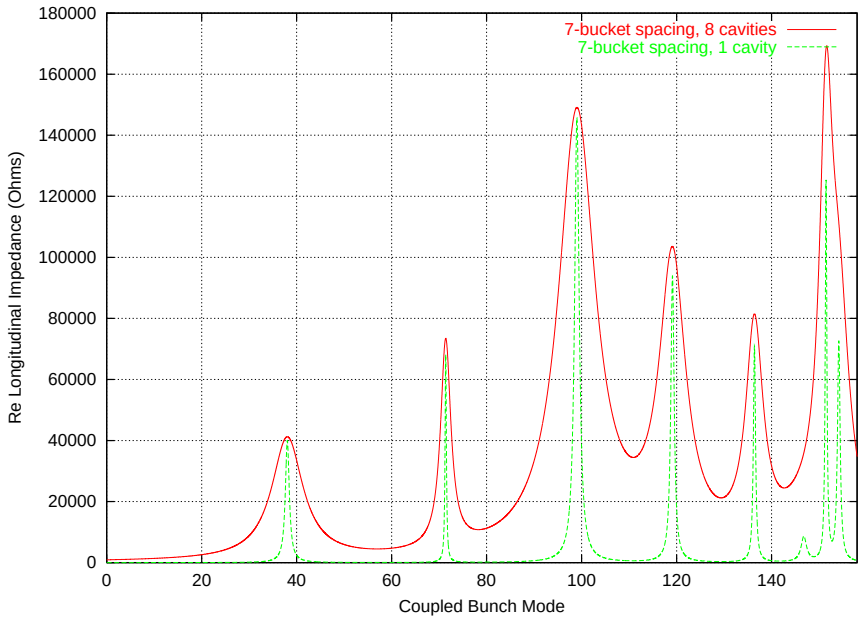

Figure 6: (color) The real part of the impedance of the higher-order parasitic resonances are plotted as a function of the coupled-bunch mode μ that they will drive. The bunches are at 7-bucket spacing. The lower (green) trace is for one cavity while the upper (red) trace corresponds to 8 cavities assuming that each resonance spread out 8 folds.

rates of Landau damping due to synchrotron frequency spread in the last row.

We see that with the number of bunches tripled and the bunch intensity increased by about 60%, coupled-bunch growth rates become very much faster. It appears that the spread in synchrotron frequency is not large enough to provide the necessary Landau damping. Obviously a fast bunch-to-bunch damper is required for the dipole mode ($m = 1$) and the quadrupole mode ($m = 2$). Some higher azimuthal modes ($m > 2$) are also unstable and cannot be damped by bunch-by-bunch dampers. To stabilize these modes and to reduce the growth rates of the dipole and quadrupole modes, one may resort to (1) passively de-Quing some annoying parasitic resonances inside the cavities and (2) increasing the bunch length. A longer bunch length will push the excitation to higher azimuthal modes, whose growth rates are usually slower and the corresponding Landau damping larger. However, longer bunches implies lower luminosity. This is especially true in the 108×108 scenario, where the bunches collide at a small angle.

Table III: Longitudinal coupled-bunch growth rates driven by the higher-order modes of the rf cavities at injection for the 108×108 scenario in Run II with rms bunch length 60 cm and bunch intensity 2.7×10^{11}.

Coupled	Growth Rate in sec^{-1}					
Bunch Mode	$m=1$	$m=2$	$m=3$	$m=4$	$m=5$	$m=6$
0	−2.676	−0.257	0.049	−0.023	−0.595	−0.638
1	−0.257	−0.603	−0.690	−0.363	−0.106	−0.020
2	−0.625	−1.208	−1.135	−0.549	−0.155	−0.029
3	−0.894	−1.726	−1.622	−0.785	−0.222	−0.041
4	−1.267	−2.403	−2.208	−1.057	−0.298	−0.055
5	−1.720	−3.085	−2.624	−1.203	−0.332	−0.060
6	−2.386	−3.885	−2.801	−1.151	−0.300	−0.053
7	−3.431	−5.133	−3.074	−1.067	−0.249	−0.041
8	−3.385	−4.937	−2.768	−0.890	−0.195	−0.031
9	−2.099	−3.117	−1.827	−0.617	−0.141	−0.023
10	−1.235	−1.901	−1.208	−0.441	−0.106	−0.018
11	−0.800	−1.284	−0.882	−0.344	−0.086	−0.015
12	−0.568	−0.948	−0.696	−0.284	−0.072	−0.012
13	−0.430	−0.741	−0.571	−0.240	−0.062	−0.011
14	−0.337	−0.596	−0.475	−0.204	−0.053	−0.009
15	−0.397	−0.356	−0.314	−0.153	−0.043	−0.008
16	−0.419	−0.239	−0.161	−0.073	−0.019	−0.003
17	−0.530	−0.247	−0.139	−0.061	−0.016	−0.003
18	−0.708	−0.275	−0.123	−0.052	−0.014	−0.002
19	−1.008	−0.337	−0.113	−0.044	−0.011	−0.002
20	−1.522	−0.457	−0.111	−0.037	−0.010	−0.002
21	−2.370	−0.666	−0.119	−0.033	−0.008	−0.001
22	−3.377	−0.917	−0.134	−0.030	−0.007	−0.001
23	−3.530	−0.949	−0.130	−0.026	−0.006	−0.001
24	−2.590	−0.680	−0.070	0.015	0.045	0.047
25	−1.657	−0.432	−0.038	0.024	0.053	0.054
26	−1.065	−0.273	−0.014	0.034	0.063	0.063
27	−0.716	−0.176	0.005	0.044	0.075	0.074
28	−0.557	−0.199	−0.124	−0.101	−0.003	0.055
29	−0.429	−0.169	−0.132	−0.114	0.000	0.066
30	−0.347	−0.153	−0.146	−0.131	0.003	0.081
31	−0.294	−0.147	−0.166	−0.153	0.007	0.101
32	−0.074	−0.100	−0.189	−0.182	0.013	0.128
33	−0.089	−0.119	−0.229	−0.222	0.021	0.164
34	−0.112	−0.146	−0.287	−0.281	0.029	0.211

Table III continued.

Coupled Bunch Mode	Growth Rate in $\sec^{-1}$					
	$m=1$	$m=2$	$m=3$	$m=4$	$m=5$	$m=6$
35	−0.146	−0.189	−0.374	−0.371	0.030	0.268
36	−0.195	−0.252	−0.504	−0.511	0.008	0.325
37	−0.280	−0.379	−0.732	−0.752	−0.077	0.353
38	−0.404	−0.574	−1.068	−1.112	−0.262	0.313
39	−0.537	−0.793	−1.430	−1.505	−0.513	0.202
40	−0.601	−0.909	−1.610	−1.704	−0.682	0.086
41	−0.553	−0.843	−1.484	−1.574	−0.668	0.026
42	−0.476	−0.751	−1.284	−1.380	−0.702	−0.130
43	−0.368	−0.588	−0.995	−1.074	−0.577	−0.141
44	−0.286	−0.465	−0.776	−0.844	−0.487	−0.154
45	−0.230	−0.382	−0.626	−0.687	−0.434	−0.174
46	−0.194	−0.330	−0.529	−0.588	−0.412	−0.201
47	−0.171	−0.301	−0.470	−0.529	−0.412	−0.235
48	−0.159	−0.289	−0.439	−0.501	−0.431	−0.276
49	−0.154	−0.291	−0.429	−0.498	−0.468	−0.327
50	−0.157	−0.305	−0.439	−0.516	−0.524	−0.389
51	−0.166	−0.332	−0.467	−0.555	−0.601	−0.467
52	−0.182	−0.372	−0.514	−0.618	−0.703	−0.565
53	−0.171	−0.378	−0.492	−0.611	−0.807	−0.705
54	−0.209	−0.463	−0.602	−0.749	−0.988	−0.863
55	−0.258	−0.572	−0.743	−0.924	−1.219	−1.065
56	−0.319	−0.707	−0.918	−1.143	−1.507	−1.317
57	−0.391	−0.866	−1.125	−1.400	−1.847	−1.613
58	−0.466	−1.033	−1.341	−1.668	−2.201	−1.922
59	−0.526	−1.167	−1.515	−1.885	−2.486	−2.170
60	−0.550	−1.220	−1.583	−1.969	−2.597	−2.266
61	−0.526	−1.166	−1.513	−1.883	−2.482	−2.165
62	−0.466	−1.032	−1.339	−1.665	−2.195	−1.914
63	−0.391	−0.866	−1.123	−1.397	−1.841	−1.605
64	−0.319	−0.707	−0.916	−1.140	−1.503	−1.309
65	−0.258	−0.572	−0.741	−0.922	−1.215	−1.059
66	−0.209	−0.463	−0.601	−0.748	−0.985	−0.858
67	−0.019	−0.374	−0.491	−0.611	−0.805	−0.701
68	0.101	−0.306	−0.405	−0.505	−0.665	−0.579
69	0.314	−0.248	−0.338	−0.422	−0.555	−0.483
70	0.781	−0.194	−0.286	−0.356	−0.469	−0.408
71	1.633	−0.137	−0.243	−0.304	−0.400	−0.348
72	1.454	−0.117	−0.210	−0.262	−0.345	−0.300

Table III continued.

Coupled	Growth Rate in $\sec^{-1}$					
Bunch Mode	$m=1$	$m=2$	$m=3$	$m=4$	$m=5$	$m=6$
73	0.676	−0.119	−0.182	−0.228	−0.300	−0.261
74	0.318	−0.112	−0.160	−0.199	−0.263	−0.228
75	0.167	−0.103	−0.141	−0.176	−0.232	−0.202
76	−0.044	−0.097	−0.126	−0.157	−0.206	−0.179
77	−0.039	−0.087	−0.112	−0.140	−0.184	−0.160
77	−0.039	−0.087	−0.112	−0.140	−0.184	−0.160
78	−0.035	−0.078	−0.101	−0.126	−0.166	−0.144
79	0.000	0.000	0.000	0.000	0.000	0.000
80	0.000	0.000	0.000	0.000	0.000	0.000
81	0.035	0.078	0.101	0.126	0.166	0.144
82	0.039	0.087	0.112	0.140	0.185	0.161
83	0.044	0.097	0.126	0.157	0.207	0.180
84	−0.168	0.103	0.141	0.176	0.232	0.202
85	−0.319	0.112	0.160	0.200	0.263	0.229
86	−0.678	0.119	0.183	0.228	0.300	0.262
87	−1.458	0.117	0.210	0.262	0.346	0.301
88	−1.630	0.138	0.244	0.305	0.401	0.350
89	−0.778	0.195	0.286	0.357	0.470	0.410
90	−0.313	0.249	0.339	0.423	0.557	0.485
91	−0.101	0.306	0.406	0.506	0.667	0.581
92	0.019	0.375	0.492	0.613	0.808	0.704
93	0.209	0.464	0.602	0.750	0.989	0.862
94	0.258	0.572	0.743	0.925	1.220	1.064
95	0.319	0.708	0.918	1.144	1.508	1.316
96	0.391	0.867	1.125	1.401	1.847	1.612
97	0.466	1.033	1.341	1.669	2.201	1.921
98	0.526	1.167	1.515	1.885	2.486	2.169
99	0.550	1.220	1.583	1.969	2.597	2.266
100	0.526	1.166	1.513	1.882	2.482	2.166
101	0.465	1.031	1.339	1.664	2.195	1.915
102	0.390	0.865	1.123	1.396	1.840	1.606
103	0.319	0.706	0.916	1.139	1.502	1.311
104	0.258	0.571	0.741	0.921	1.214	1.060
105	0.209	0.463	0.601	0.746	0.984	0.859
106	0.171	0.378	0.491	0.610	0.804	0.702
107	0.182	0.372	0.514	0.617	0.701	0.562
108	0.166	0.331	0.466	0.554	0.599	0.465
109	0.157	0.305	0.439	0.515	0.523	0.388

Table III continued.

Coupled Bunch Mode	Growth Rate in $\sec^{-1}$					
	$m=1$	$m=2$	$m=3$	$m=4$	$m=5$	$m=6$
110	0.154	0.291	0.429	0.498	0.468	0.326
111	0.159	0.289	0.439	0.501	0.431	0.275
112	0.171	0.302	0.470	0.530	0.412	0.234
113	0.194	0.331	0.530	0.589	0.412	0.200
114	0.230	0.383	0.627	0.689	0.435	0.174
115	0.287	0.465	0.778	0.847	0.488	0.154
116	0.369	0.589	0.998	1.078	0.579	0.140
117	0.477	0.752	1.287	1.385	0.704	0.130
118	0.554	0.844	1.486	1.578	0.670	−0.026
119	0.601	0.908	1.610	1.703	0.681	−0.088
120	0.536	0.792	1.427	1.500	0.509	−0.205
121	0.404	0.573	1.064	1.106	0.258	−0.315
122	0.280	0.378	0.729	0.748	0.074	−0.353
123	0.194	0.251	0.502	0.508	−0.009	−0.324
124	0.146	0.189	0.373	0.369	−0.030	−0.266
125	0.112	0.146	0.286	0.280	−0.028	−0.210
126	0.089	0.118	0.228	0.222	−0.021	−0.163
127	0.074	0.100	0.189	0.181	−0.013	−0.127
128	0.294	0.147	0.165	0.152	−0.007	−0.101
129	0.347	0.153	0.146	0.130	−0.003	−0.081
130	0.429	0.170	0.132	0.114	0.000	−0.066
131	0.558	0.199	0.124	0.101	0.003	−0.054
132	0.717	0.176	−0.004	−0.044	−0.075	−0.073
133	1.067	0.274	0.014	−0.034	−0.063	−0.063
134	1.659	0.434	0.038	−0.024	−0.053	−0.054
135	2.594	0.682	0.070	−0.015	−0.045	−0.047
136	3.532	0.950	0.130	0.026	0.006	0.001
137	3.374	0.916	0.134	0.030	0.007	0.001
138	2.366	0.664	0.119	0.033	0.008	0.001
139	1.520	0.456	0.111	0.038	0.010	0.002
140	1.006	0.336	0.113	0.044	0.011	0.002
141	0.708	0.274	0.123	0.052	0.014	0.002
142	0.529	0.247	0.139	0.062	0.016	0.003
143	0.419	0.239	0.161	0.073	0.019	0.003
144	0.397	0.356	0.314	0.154	0.043	0.008
145	0.337	0.597	0.476	0.204	0.053	0.009
146	0.430	0.742	0.572	0.241	0.062	0.011
147	0.569	0.950	0.697	0.285	0.073	0.012

Table III continued.

Coupled	Growth Rate in $\sec^{-1}$					
Bunch Mode	$m=1$	$m=2$	$m=3$	$m=4$	$m=5$	$m=6$
148	0.801	1.287	0.885	0.345	0.086	0.015
149	1.237	1.908	1.213	0.443	0.106	0.018
150	2.103	3.129	1.836	0.621	0.141	0.023
151	3.389	4.949	2.777	0.894	0.196	0.031
152	3.427	5.125	3.071	1.069	0.250	0.042
153	2.383	3.877	2.799	1.152	0.301	0.053
154	1.718	3.080	2.621	1.203	0.332	0.060
155	1.265	2.397	2.202	1.053	0.296	0.054
156	0.893	1.721	1.616	0.781	0.221	0.041
157	0.625	1.205	1.131	0.547	0.154	0.028
158	0.257	0.601	0.687	0.361	0.106	0.020
Laudau Damping rate (s^{-1})						
	0.336	0.475	0.581	0.671	0.751	0.822

2 TRANSVERSE COUPLED-BUNCH INSTABILITIES

2.1 RESISTIVE WALL

A most serious transverse coupled-bunch instability in a storage ring may be driven by the resistive wall. If there are M_s identical equally spaced bunches in the ring, there are $\mu = 0, \cdots, M_s - 1$ transverse coupled modes when the center-of-mass of one bunch leads its predecessor by the betatron phase of $2\pi\mu/M_s$. At the same time, each bunch can execute longitudinal motion with $m = 0, 1, \cdots$ nodes. The growth rate for the mode μm is [4]

$$\frac{1}{\tau_{\mu m}} = -\frac{1}{1+m}\frac{eMI_b c}{4\pi\nu_\beta E}\sum_k \mathcal{R}e\, Z_\perp[(kM_s + \mu + \nu_\beta + m\nu_s)\omega_0]F'_m(\omega\tau_{_L} - \chi)\ , \qquad (2.1)$$

where M is the number of bunches. Strictly speaking Eq. (2.1) is correct only if $M = M_s$ or a completely filled ring. For example, in the 36×36 scenario with 1.7×10^{11} particles per bunch and rms bunch length 60 cm, the bunch spacing is 21 buckets; therefore $M = 36$ and $M_s = H/21 = 53$. On the other hand, in the 108×108 scenario with 7-bucket spacing, 2.7×10^{11} particles per bunch and rms bunch length 50 cm, $M = 108$ and $M_s = 1113/7 = 159$. There are many unfilled buckets in both scenarios; thus Eq. (2.1) will not be an accurate description

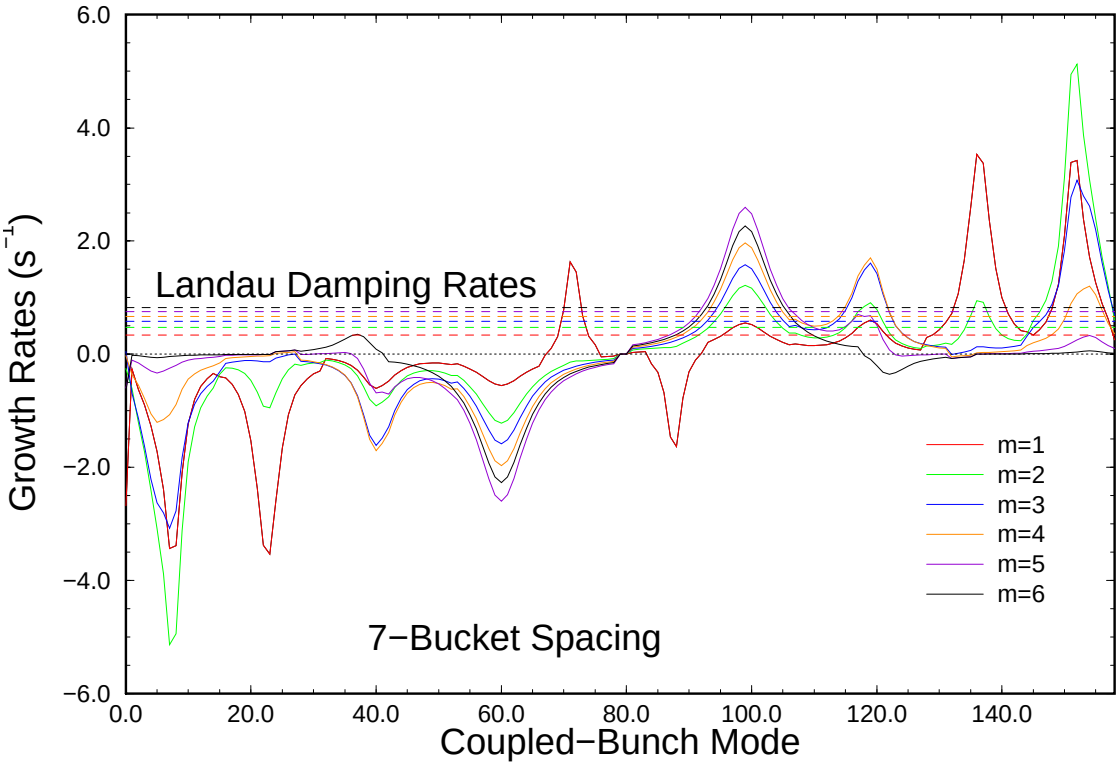

Figure 7: (color) Plot of growth rates (positive) and damping rates (negative) of each coupled-bunch mode driven by the higher-order parasitic resonances of the 8 Tevatron cavities. The bunch spacing is 7 buckets. The Landau damping rates are shown in dashes.

of the beam dynamics.

As the frequency $\omega \to \pm 0$, the real part of the resistive-wall impedance approaches first $\pm|\omega|^{-1/2}$, then $|\omega|^{-1}$ when the skin depth exceeds the thickness of the pipe wall, and finally zero when the frequency is exactly zero. At the residual betatron tune of the Tevatron, $[\nu_\beta] \sim 0.57$, we are in the regime of $\pm|\omega|^{-1/2}$ dependency. Therefore, there is always a mode μ that corresponds to a large negative $\mathcal{R}e\, Z_\perp$ and drives the transverse coupled-bunch instability. For example, with the betatron tune $\nu_\beta = 20.57$, mode $\mu = 53 - 21 = 32$ ($\mu = 159 - 21 = 138$ for the 108-by-108 scenario) or frequency $-0.43\,\omega_0/(2\pi)$ with $k = 0$ in the summation of Eq. (2.1) contributes the largest negative $\mathcal{R}e\, Z_\perp$, which is -66.70 MΩ/m according to our former estimate made in Ref. [5]. The next contribution with $k = 1$ will give $\mathcal{R}e\, Z_\perp = +6.03$ MΩ/m in the 36×36 scenario and $+3.47$ MΩ/m for protons in the 108×108 scenario. The average current per bunch is $I_b = 1.300$ mA for the first scenario and 2.064 mA for the second. The growth rate is therefore given mostly by the $k = 0$ term in the summation

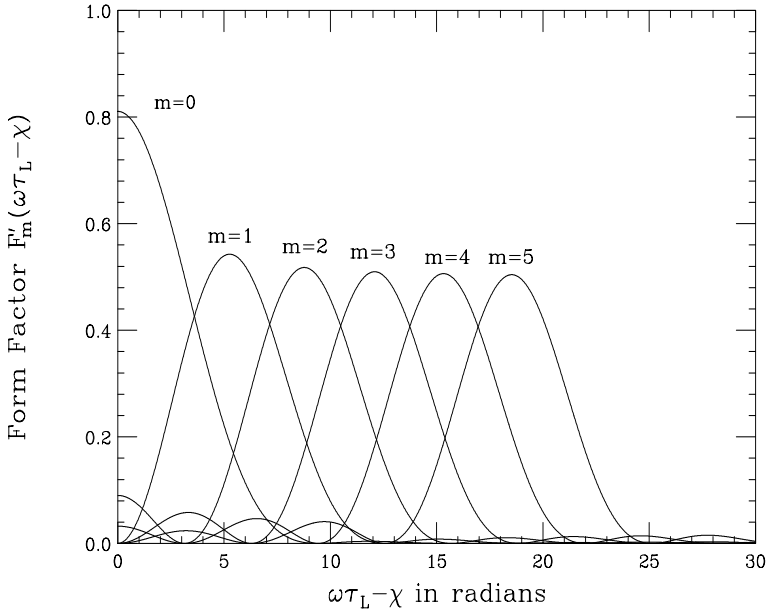

Figure 8: Plot of form factor $F'_m(\omega\tau_{_L}-\chi)$ for modes $m = 0$ to 5. With the normalization in Eq. (2.3), these are exactly the power spectra h_m.

and is very insensitive to the choice of M_s in Eq. (2.1). For such a low driving frequency, only the lowest longitudinal mode $m = 0$ will be excited. The growth rates after doing the actual summations are 19.5 and 93.2 s^{-1}, respectively, for the two scenarios. Modes $\mu = 31$, 30, 29, $\cdots$ ($\mu = 137,\ 136,\ 135,\ \cdots$ for the 108-by-108 scenario) are also unstable; the growth rates are, respectively, 10.6, 8.0, 6.6, $\cdots$ s^{-1}, and 51.0, 39.0, 32.8, $\cdots$ s^{-1} for the two operating scenarios. The computation has been performed at zero chromaticity ($\xi = 0$), so that the chromatic phase $\chi = \xi\omega_0\tau_{_L}/\eta = 0$. Also, we have used the form factor $F'_0(0) = 8/\pi^2 \approx 0.811$, where, for convenience, Sacherer's sinusoidal modes of excitation have been assumed. These growth rates are much larger than those in Run I because there are more bunches. If one operates at chromaticity $\xi = +6$, $\chi = 5.69$ and $F'_0(5.69) \approx 0.142$ from Fig. 8 for the first scenario, while $\chi = 4.75$ and $F'_0(5.69) \approx 0.255$ for the second scenario. The growth rates for $\mu = 32$ (or 138) drop to 3.42 and 29.3 s^{-1}, respectively, which can be damped by a tune spread. For example, a tune spread of $\Delta\nu_\beta = 0.0001$ will lead to a spread of betatron angular frequency of $\Delta\nu_\beta\omega_0 = 30$ s^{-1}, and will damp a growth rate up to ~ 17.0 s^{-1} (FWHM for a Gaussian spread) [4]. For further discussion, we need to study the sinusoidal modes of excitation in the next subsection.

2.2 SINUSOIDAL MODES

The Sacherer's sinusoidal modes of excitation consist of the orthonormal set

$$p_m(\tau) = \begin{cases} \cos(m+1)\pi\dfrac{\tau}{\tau_{_L}} & m = 0, 2, \cdots, \\ \sin(m+1)\pi\dfrac{\tau}{\tau_{_L}} & m = 1, 3, \cdots, \end{cases} \tag{2.2}$$

such that $p_m(\tau)$ has m nodes along the bunch not including the ends. The power spectrum is proportional to

$$h_m(\omega) = \frac{4(m+1)^2}{\pi^2}\,\frac{1+(-1)^m\cos\pi y}{[y^2-(m+1)^2]^2}\ , \tag{2.3}$$

where $y = \omega\tau_{_L}/\pi$ and $\omega = kM_s - \mu + \nu_\beta + m\nu_s - \chi/\tau_{_L}$. They are plotted in Fig. 9. The normalization of $h_m(\omega)$ in Eq. (2.3) has been chosen in such a way that, when the smooth approximation is applied to the summation over k, we have

$$B\sum_{k=-\infty}^{+\infty} h_m(\omega) \approx \frac{B}{M_s\omega_0}\int_{-\infty}^{+\infty} h_m(\omega)d\omega = 1\ . \tag{2.4}$$

Here $B = M_s\omega_0\tau_{_L}/(2\pi)$ is the bunching factor, or the ratio of full bunch length to bunch separation. Then the form factor $F'_m(\omega)$ in Eq. (2.1) just equals $h_m(\omega)$.

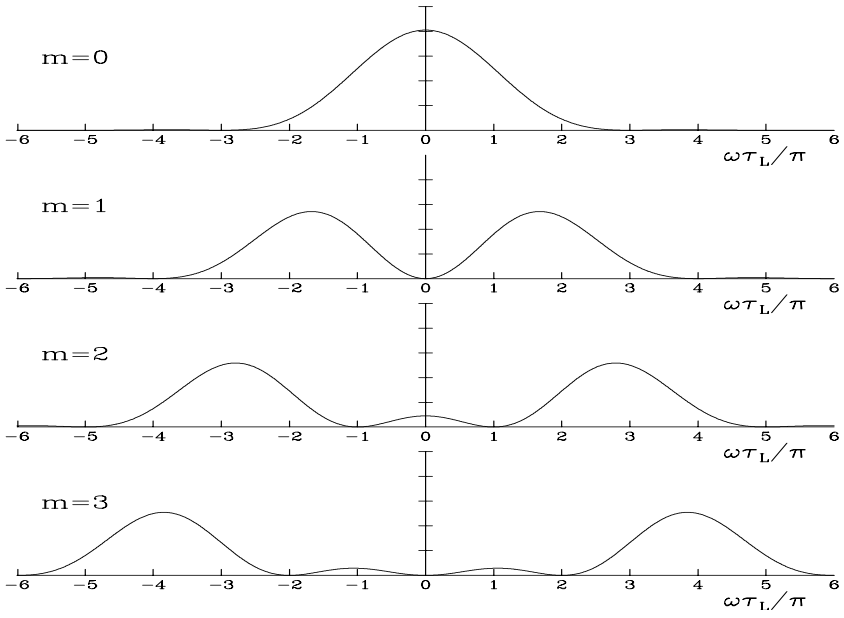

Figure 9: Power spectra $h_m(\omega)$ for modes $m = 0$ to 3 with zero chromaticity.

The Sacherer integral equation for transverse instability is an eigen-value-eigen-function problem when the unperturbed longitudinal distribution $g_0(r)$ in the longitudinal phase space is given. Physically, the modes of excitation $p_m(\tau)$ are the projection of the eigen-functions in the longitudinal phase space onto the time axis. The sinusoidal modes correspond to the water-bag distribution in phase space, so that the linear distribution is

$$\rho(\tau) \propto \sqrt{\hat{\tau}^2 - \tau^2} \ . \tag{2.5}$$

For the distribution $g_0(r) \propto (\hat{\tau}^2 - r^2)^{-1/2}$ in the longitudinal phase space, $p_m(\tau)$ are the Legendre polynomials and the Fourier transforms the spherical Bessel functions j_m. When $g_0(r)$ is bi-Gaussian, $p_m(\tau)$ are Hermite polynomials. Sometimes the growth rates computed are rather sensitive to the longitudinal bunch distribution assumed. Therefore, results in this section are estimates only.

We now learn that a chromaticity of $\xi = \eta/(f_0\tau_{_L}) = +10.73$ will push the power spectra in Fig. 9 to the right (or positive frequency side) by two $\omega\tau_{_L}/\pi$ units. The $m=0$ will then only see the positive-frequency impedance and no instability will result. However, the $m = 1$ mode will now peak at zero frequency and the resistive wall impedance will drive the $m = 1$ mode unstable and a quadrupole transverse damper will be required, if Landau damping coming from tune spread is not large enough.

2.3 TRANSVERSE COUPLED-BUNCH INSTABILITY DRIVEN BY RESONANCES

The narrow transverse resonant modes of the rf cavities will also drive transverse coupled-bunch instability. The growth rate is described by the general growth formula of Eq. (2.1). When the resonance is narrow enough, only one frequency $-\omega_r/(2\pi)$ contributes in the summation. Thus the growth rate becomes

$$\frac{1}{\tau_{\mu m}} = -\frac{1}{1+m}\frac{eMI_bc}{4\pi\nu_\beta E}\,\mathcal{R}e\, Z_\perp(\omega_r)F'_m(\omega_r\tau_{_L}-\chi) \ , \tag{2.6}$$

where M is the number of bunches and the frequency ω_r is negative.

There have not been any measurements for the dipole modes in the rf cavities, and we need to rely on the URMEL results, which are listed in Table IV. The contribution of all the resonances to the 53 coupled-bunch modes in the 36-by-36 scenario is shown in Fig. 10.

Table IV: Transverse modes for one whole cavity.

Mode Type	Frequency (MHz)	R/Q (Ω/m)	Q
1-EE-1	486.488	229.80	31605
1-ME-2	486.864	148.95	31487
1-EE-2	513.370	117.38	33262
1-ME-3	518.317	117.93	34008
1-EE-3	561.727	81.62	33029
1-ME-4	575.298	3.84	35810
1-EE-4	625.123	61.00	32598
1-ME-5	650.853	35.21	37592
1-EE-5	699.723	54.76	33407

Because we are looking at negative frequencies, the real part of the transverse impedance is negative. The upper trace is for one cavity while the lower trace for 8 cavities again assuming 8-fold de-Quing. Together with each coupled-bunch mode μ, certain longitudinal azimuthal modes m will be excited and transverse oscillations along the bunch will be observed. These azimuthal modes are usually called head-tail modes. As it will be shown later that the growth rates for various modes are small, we do not compute the growth rates for all the modes. Instead, we compute only the fastest growing modes excited by each resonance. The results are listed in Table V for the 36-by-36 scenario.

Some comments are in order. Here, we assume that the higher-order modes of the 8 rf cavities do not fall on top of each other at exactly the same frequencies. Instead, we assume that the resonances summed over 8 cavities will be de-Qued 8 times and the shunt impedance corresponding to a certain resonance will be the same as that for a single cavity. At the same time, we assume that a peak of a resonance, when summed over the 8 rf cavities, falls exactly on top of a particular synchrotron sideband of the betatron line.[§] The frequencies of the lowest 9 higher-order modes range from 486.5 to 699.7 MHz. Therefore $\omega_r\tau_{_L}/\pi - \chi/\pi$ (ω_r is negative) for the 36-by-36 scenario ranges from -8.7 to -12.5 at zero chromaticity. From the power spectra in Fig. 9, this implies modes roughly from $m = 8$ to 11 will be excited. These are listed in column 4 of the table. We can see in Table V that the growth rates actually peak for these modes. Since the growth rates are affected so much by the mode of excitation, we also give the *bare* growth rate for each resonance in column 5 when the form factor F'_m and

[§]This assures the fastest growth rates.

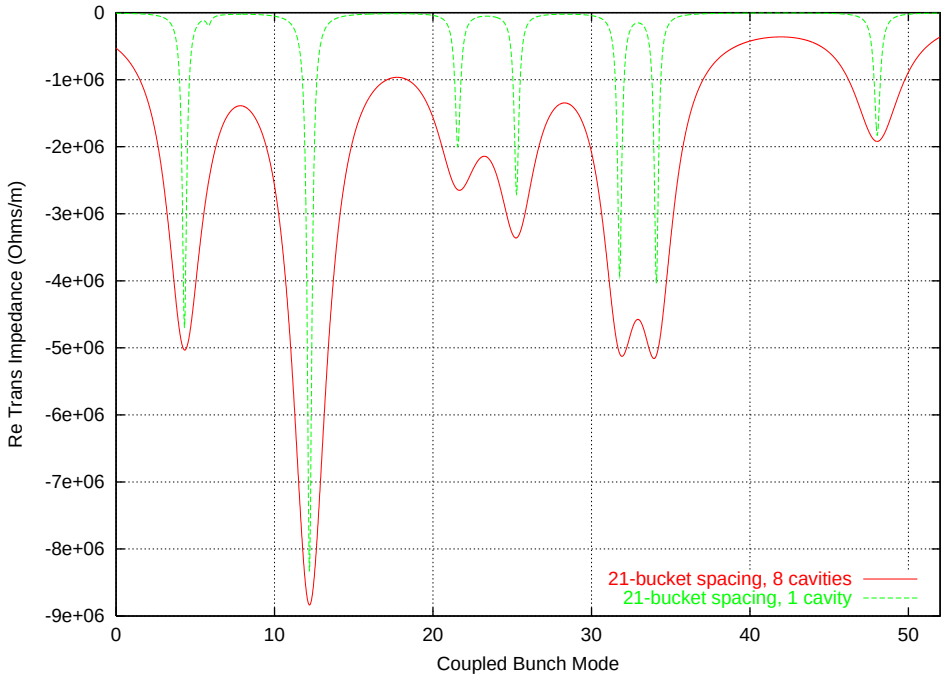

Figure 10: (color) The real part of the transverse impedance of the higher-order dipole resonances are plotted as a function of the coupled-bunch mode μ that they will drive. The upper (green) trace is for one cavity while the lower (red) trace corresponds to 8 cavities assuming that each resonance spreads out 8 folds. The bunch spacing is 21 buckets.

Table V: Growth rates for transverse coupled-bunch modes driven by higher-order dipole modes of the rf cavities in the 36×36 scenario. The fastest growth rate driven by each higher-order dipole mode is underlined.

f_r	R_s	Q	$m_{\rm pk}$	Growth Rate (s^{-1})								Coupled
MHz	Ω/m			Growth	$m=5$	$m=6$	$m=7$	$m=8$	$m=9$	$m=10$	$m=11$	Mode μ
Chromaticity $\xi = 0$												
486.5	7262	31605	7.7	2.627	0.006	0.004	0.098	<u>0.141</u>	0.029	0.002	0.004	12
486.9	4689	31487	7.7	1.696	0.004	0.002	0.063	<u>0.091</u>	0.019	0.001	0.003	4
513.4	3904	33262	8.2	1.412	0.003	0.001	0.020	<u>0.075</u>	0.043	0.001	0.004	32
518.3	4010	34008	8.3	1.451	0.002	0.001	0.016	<u>0.073</u>	0.050	0.002	0.003	34
561.7	2695	33029	9.1	0.975	0.000	0.002	0.000	0.017	<u>0.048</u>	0.022	0.000	25
575.3	137	35810	9.3	0.050	0.000	0.000	0.000	0.000	<u>0.002</u>	0.002	0.000	6
625.1	1988	32598	10.2	0.719	0.000	0.000	0.001	0.000	0.008	<u>0.031</u>	0.018	22
650.9	1323	37592	10.7	0.479	0.000	0.000	0.000	0.001	0.001	0.014	<u>0.019</u>	12
699.7	1829	33407	11.5	0.662	0.000	0.000	0.000	0.000	0.001	0.002	<u>0.021</u>	48

the factor $(1+m)^{-1}$ are not included. Increasing the chromaticity shifts the mode spectra of the bunch to the right (positive frequency side); so head-tail modes of much higher m will be excited. On the other hand, running the Tevatron at negative chromaticities will shift the bunch mode spectra to the right. and head-tail modes with lower m will be excited instead. As a whole, the growth rates are extremely slow. A tune spread of $\Delta\nu_\beta = 0.0001$, for example, will damp a growth rate up to ~ 17 s^{-1}.

We next look at the 108-by-108 scenario. For the symmetrically filled ring with 7-bucket spacing, there are 159 coupled-bunch modes. The real parts of the transverse impedance contributing to these modes are depicted in Fig. 11. The upper trace is for one cavity while the lower trace for 8 cavities again assuming 8-fold de-Quing. Again, we compute only the fastest growing modes driven by individual resonances. The results are listed in Table VI.

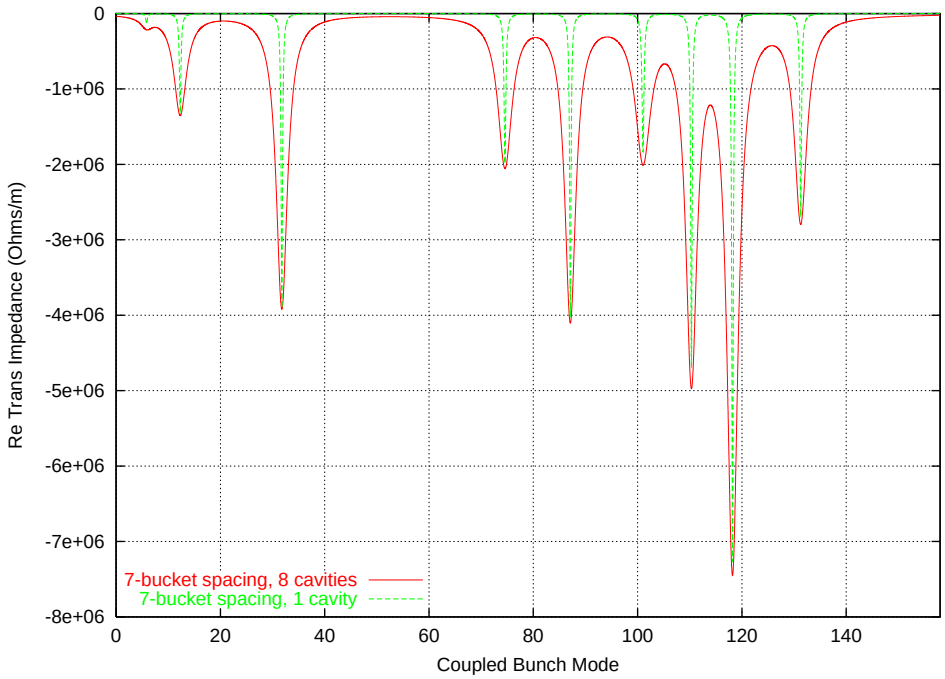

Figure 11: (color) The real part of the transverse impedance of the higher-order dipole resonances are plotted as a function of the coupled-bunch mode μ that they will drive. The upper (green) trace is for one cavity while the lower (red) trace corresponds to 8 cavities assuming that each resonance spreads out 8 folds. The bunch spacing is 21 buckets.

In this scenario, because of the shorter bunch length $|\omega_r \tau_{_L}/\pi|$ will be smaller and modes $m = 6$ to 9 will be driven instead. These are shown in Table VI. Due to the presence of more bunches, high bunch intensity, and short bunch length, the growth rates are relatively faster

Table VI: Growth rates for transverse coupled-bunch modes driven by higher-order dipole modes of the rf cavities in the 108×108 scenario. The fastest growth rate driven by each higher-order dipole mode is underlined.

f_r	R_s	Q	$m_{\rm pk}$	Growth Rate (s^{-1})								Coupled
MHz	Ω/m			Growth	$m=5$	$m=6$	$m=7$	$m=8$	$m=9$	$m=10$	$m=11$	Mode μ
Chromaticity $\xi = 0$												
486.5	7262	31605	6.3	12.518	0.185	<u>0.816</u>	0.534	0.018	0.038	0.004	0.012	118
486.9	4689	31487	6.3	8.083	0.118	<u>0.525</u>	0.347	0.012	0.025	0.002	0.008	110
513.4	3904	33262	6.7	6.729	0.017	0.303	<u>0.399</u>	0.073	0.008	0.011	0.002	32
518.3	4010	34008	6.7	6.912	0.010	0.281	<u>0.421</u>	0.093	0.006	0.014	0.002	87
561.7	2695	33029	7.4	4.646	0.006	0.040	<u>0.246</u>	0.200	0.013	0.011	0.003	131
575.3	137	35810	7.6	0.237	0.001	0.001	0.010	<u>0.012</u>	0.002	0.000	0.000	6
625.1	1988	32598	8.3	3.427	0.005	0.003	0.032	<u>0.168</u>	0.124	0.006	0.008	75
650.9	1323	37592	8.7	2.281	0.001	0.005	0.003	0.076	<u>0.110</u>	0.023	0.002	12
699.7	1829	33407	9.4	3.153	0.001	0.003	0.004	0.018	<u>0.129</u>	0.116	0.010	101

than those for the 36-by-36 scenario. The fastest growth rate shown is 0.816 s^{-1}, which will be damped by a small betatron tune spread. As a whole, transverse coupled-bunch instabilities driven by the higher-order modes in the rf cavities should not represent a problem at all.

References

[1] F.J. Sacherer, IEEE Trans. Nuclear Sci. **NS 20**, 3, 825 (1973).

[2] D. Sun, private communication.

[3] See for example, K.L.F. Bane, P.B. Wilson, and T. Weiland, *AIP Proc. 127, Phys. of High Energy Accel.,* BNL/SUNY, 1983, p.875.

[4] F.J. Sacherer, *Theoretical Aspects of the Behaviour of Beams in Accelerators and Storage Rings*, Proc. First Course of Int. School of Part. Accel., Erice, Nov. 10-22, 1976, p.198.

[5] K.Y. Ng, *Impedances and Collective Instabilities of the Tevatron at Run II*, Fermilab Report TM-2055, 1998.